Echo in complex networks

Richa Phogat,[1] Sudeshna Sinha,[1,2] and P. Parmananda[1]
[1]*Department of Physics, Indian Institute of Technology, Bombay, Powai, Mumbai 400 076, India*
[2]*Department of Physical Sciences, Indian Institute of Science Education and Research Mohali, Knowledge City, SAS Nagar, Sector 81, Manauli, P.O. Box 140306, Punjab, India*

(Received 12 November 2019; accepted 4 February 2020; published 21 February 2020)

Large populations of globally coupled or uncoupled oscillators have been recently shown to exhibit an intriguing echo behavior [Ott, Platig, Antonsen, and Girvan, Chaos: An Interdiscip. J. Nonlinear Sci. **18**, 037115 (2008); Chen, Tinsley, Ott, and Showalter, Phys. Rev. X **6**, 041054 (2016)], wherein a system is perturbed by two successive pulses at times T and $T+\tau$ inducing a spontaneous increase in the order parameter at the given times. These two provoked increments in the order parameter are followed by an unprovoked spontaneous increment in the order parameter at time $T+2\tau$ termed as an *echo*. In this paper, the effects of network topology on the emergence of an echo are explored. Two principal network parameters, namely, average degree and network randomness, are varied for this purpose. The networks are rewired to increase randomness in the network connections using the Watts-Strogatz algorithm to generate small world networks [Watts and Strogatz, Nature (London) **393**, 440 (1998)]. Thus, the whole span of networks ranging from a regular ring to a completely random network is explored. The average degree of the underlying connectivity, starting from nearest neighbor connections, is also monotonically increased and its effects on the echo behavior are analyzed. We find that for rings with low average degrees and high coupling strengths a discernible echo is not observed. Remarkably, an echo reemerges in the presence of sufficient randomness in the connections for such networks. For a regular ring network, increasing the average degree after a critical value also yields a transition to echo behavior. However, for completely random networks echoes are present in networks of all average degrees. This suggests that randomizing connections can induce echoes in systems even when the average degree of connections is very low. Another subtle feature arises for intermediate randomness, where the system exhibits a nonmonotonic dependence of the echo size on average degree. The echo size was found to be minimum at an intermediate value of the average degree. Lastly we consider the influence of dynamically changing links on the echo size and demonstrate that time-varying connections destroy the echo in low average degree networks, while the echo persists under dynamic links in high average degree networks. So our results clearly demarcate the class of networks that are robust candidates for exhibiting echoes, as well as provide caveats for the observation of echoes in networks.

DOI: 10.1103/PhysRevE.101.022216

I. INTRODUCTION

Networks of coupled oscillators manifest a variety of complex dynamical behaviors [1,2], such as chimera states observed in identical oscillators [3–7] and amplitude or oscillation death [8–11]. Extended perturbations to an ensemble of oscillators may lead to entrainment [12,13], enhanced reliability [14], suppression of temporal and spatiotemporal disorder [15], bistability [16], antiperiodic oscillations [17], stochastic resonance [18], and pattern formation [19,20]. An intriguing addition to the class of spatiotemporal patterns is the echo behavior observed in populations of coupled or uncoupled oscillators [21,22]. During the echo phenomenon, a system is perturbed using two successive pulses separated by a time τ. Phase resetting [21,22] of the oscillators as a consequence of these pulses causes an increase in the order parameter. A spontaneous unperturbed increment in the order parameter may appear at a time τ after the second perturbation and is termed as an *echo*. Subsequent echoes may also be observed at times $n\tau$ ($n>1$) after the second pulse. This counterintuitive effect has been reported in both theoretical [21,23–25] and experimental studies [22]. In this paper we explore how the emergence of an echo is influenced by network topology. As a test bed of our investigation, we consider a network of phase oscillators, where varying degrees of randomness are introduced in network connections by using the Watts-Strogatz algorithm to generate small world networks [26]. The smallest average degree for a ring network is taken to be 2, i.e., every oscillator is connected to two nearest neighbors. These nearest neighbor connections are symmetrically increased to augment the average degree of the network. Monotonically increasing the randomness in networks of varying average degrees covers a comprehensive set of networks showing a plethora of interesting dynamical behaviors. Introducing randomness in the network connections as proposed in [26] induces spatiotemporal synchronization [27], which was not possible in the case of strictly nearest neighbor connections. Also, keeping the randomness in network connections constant and changing the links at different frequencies, it was observed that at fast rewiring frequencies spatiotemporal regularity of a network of coupled maps is enhanced [28]. The mechanisms of large scale integration that enable the emergence of coherent behavior and cognition are also argued to be caused by the formation of dynamic links [29–31].

Given the ubiquity of such networks in nature, ranging from brain functional networks [32] to metabolic networks [33] to social networks [34], in our opinion, it would be of potential interest to explore the effects of these network topologies on echo behavior. The organization of this paper is as follows. In Sec. II, a brief description of the model is presented and the dependence of echo size on coupling strength is analyzed. In Sec. III, dependence of echo size on randomness and average degree of the network is explored for the case of networks where the connections between the oscillators are static. The emergence of echoes in time-varying networks with dynamically changing links is considered in Sec. IV. The salient features of the results are summarized with some potential applications in Sec. V.

II. MODEL OF COUPLED PHASE OSCILLATORS

In this paper, we focus on an ensemble of phase oscillators coupled via the Watts-Strogatz algorithm [26]. The topology of the connectivity network is determined by two principal control parameters. The first significant parameter is the average degree, denoted by $\langle d \rangle$, defined as the average number of connections an oscillator forms with other oscillators. A network of high average degree indicates that these oscillators, on average, are coupled to a larger set of oscillators. In a regular ring network of average degree d_0, each oscillator has $d_0/2$ nearest neighbor connections on either side. The other important network parameter quantifies the randomness of the network connections, denoted by β. In the Watts-Strogatz [26] algorithm, on average, each link is rewired randomly with a probability β. Hence, this parameter allows one to transition smoothly from a regular ring ($\beta = 0$) of a particular average degree to a completely random network ($\beta = 1$) with the same average degree.

The dynamical equation of a phase oscillator in such a network is given as follows:

$$\frac{d\theta_i}{dt} = \omega_i + \frac{C_0}{\langle d \rangle} \sum_j A_{ij} \sin(\theta_j - \theta_i) \;\; \forall \;\; j \neq i \qquad (1)$$

where θ_i represents the phase of the ith oscillator and ω_i represents the intrinsic frequency of the ith oscillator. N is the total number of oscillators in the ensemble with the average degree of the network being equal to $\langle d \rangle$. The average degree of this network is defined as $\langle d \rangle = \frac{\sum_i \sum_j A_{ij}}{N}$. A_{ij} is an element of the adjacency matrix reflecting the link between the ith and jth oscillator, with $A_{ij} = 1$ if a connection exists between oscillator i and j, and zero otherwise. For oscillators coupled on a ring of average degree $\langle d \rangle$, matrix A is a banded circulant matrix with $A_{ij} = 1$, $\forall \; i - \frac{d}{2} \leqslant j \leqslant i + \frac{d}{2}$ where $j \neq i$ and zero otherwise. For the work presented here, the intrinsic frequencies are taken to be linearly proportional to the site index i. Specifically, with no loss of generality, we consider $\omega_i = 20 + \frac{10(i-1)}{N-1}$, with $N = 2000$. C_0 denotes the coupling constant and is fixed at 0.5 unless specified otherwise. All the integrations were performed using Euler's method with a sufficiently small step size. The coupling between the oscillators is bidirectional and during the randomization of the networks using the Watts-Strogatz [26] algorithm no nodes become isolated. However, there is a finite probability of forming subnetworks which may be disconnected from each other at very low average degrees ($\langle d \rangle = 2$). As mentioned in [26], a network is guaranteed to be completely connected only when $\langle d \rangle \gg ln(N)$. This implies, in the context of the present paper, that there is a finite probability of a network not being completely connected for $\langle d \rangle < ln(N) = 7.6$. Nonetheless, the central theme of this paper is echo behavior, which has been shown to exist even for uncoupled networks [22], and hence these very low degree networks are also explored in the present paper.

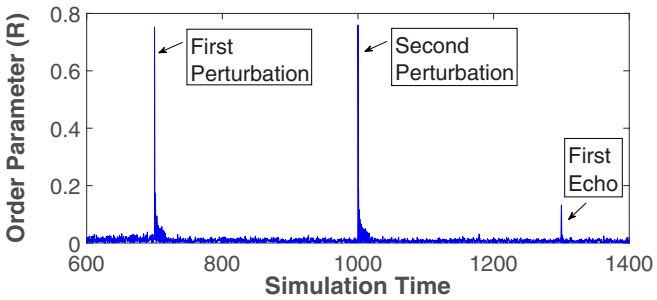

FIG. 1. System response to the two perturbations given at $T = 700$ time units and $T + \tau = 1000$ time units, where $\tau = 300$ time units. The unprovoked spontaneous rise in order parameter at $T + 2\tau = 1300$ time units is the first echo.

Figure 1 shows the quintessential echo behavior as observed in a ring ($\beta = 0$) of 2000 oscillators with average degree, $\langle d \rangle = 200$. The order parameter R for the system is calculated as

$$R(t) = \left| \frac{\sum_{i=1}^{N} e^{\iota \theta_i(t)}}{N} \right|. \qquad (2)$$

Applying a perturbation to the system momentarily resets the phases of all the oscillators lying in the phase domain $[0.8\pi : 2\pi]$ to zero. This leads to a spontaneous increment in the order parameter. Two such perturbations were applied on the aforementioned network at time T (700 time units) and $T + \tau$ (1000 time units). It is evident from the system response that after two successive perturbations at T and $T + \tau$ there is an unprovoked spontaneous rise in the order parameter at $T + 2\tau$ (1300 time units). So, in Fig. 1, the first echo is clearly discernible in this ring of phase oscillators.

The appearance of echo in Zhabotinsky-Bucholtz-Kiyatkin-Epstein model simulations has been explained using the phase versus frequency plot in [22]. The authors elaborated the emergence of echo by plotting the phase of the oscillator as a function of oscillator frequency at six different time stamps. To revisit the arguments given in [22], the behavior of the phases of the oscillators in response to the two perturbations, and at the time of the echo, is explored. Figure 2 shows the phase distribution of all the oscillators of the network as a function of their frequency at six different time stamps. This figure was plotted for the same system as shown in Fig. 1, i.e., for the case of 2000 phase oscillators in a ring of average degree 200. The oscillators are uniformly distributed in the frequency-phase plot before the first perturbation was applied at $T = 700$ time units [panel (a)]. This perturbation resets the oscillators lying in the

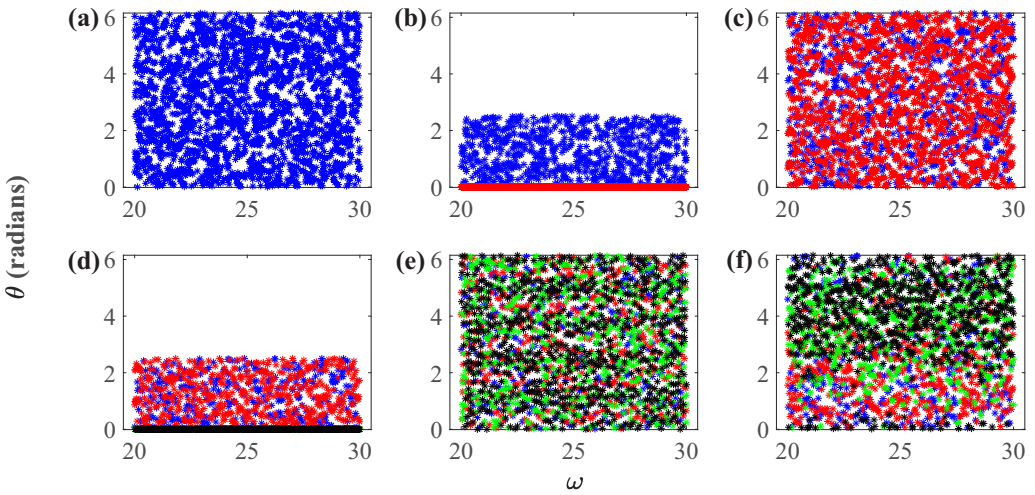

FIG. 2. Phase θ as a function of oscillator frequency (ω) at six different time stamps. (a) The phases of the oscillators are uniformly distributed before the first perturbation, which amounts to a low order parameter ($T < T_{p1}$). (b) At the first perturbation, i.e., $T = T_{p1} = 700$ time units, the phases of the oscillators lying in the $[0.8\pi : 2\pi]$ region are reset to zero. This leads to an increment in the order parameter of the system. The oscillators reset by the first perturbation are color coded to be red while the rest are blue. This gives rise to two groups of oscillators. Group I was not reset by the first perturbation and group II was reset by the first perturbation. (c) All the phases were again uniformly distributed before the second perturbation ($T < T_{p2}$). (d) Applying the second perturbation at $T_{p2} = T_{p1} + \tau = 1000$ time units generates four groups, color coded to be blue, red, green, and black. In these four groups, the information regarding the frequency (ω) distribution of each group is embedded. This frequency distribution of four groups is such that it leads to a small gathering of phases at the time of the echo. This reflects as an increment in the order parameter. The lower middle (e) and lower right (f) panel compare the distribution of phases at a time long before the echo and at the time of the echo ($T = T_{\text{echo}} = 1300$ time units), respectively. The phase gathering is noticeable at the time of the echo.

$[0.8\pi : 2\pi]$ phase domain to zero [panel (b)]. This resetting creates two groups of oscillators: (a) group I, which was not reset by the first perturbation and is color coded to be blue, and (b) group II, which was reset by the first perturbation and is color coded to be red. The phase distribution as shown in panel (c) is uniform again before the next perturbation was applied at $T + \tau = 1000$ time units. This second perturbation creates four groups [panel (d)]: group I (blue), which was not reset by either of the perturbations; group II (red), which was reset by the first perturbation but not the second; group III (green), which was reset by the second perturbation and not the first; and group IV (black), which was reset by both the perturbations. Being reset by a perturbation implies the presence of oscillators in the $[0.8\pi : 2\pi]$ region. Not being reset limits the oscillators to the phase region $[0 : 0.8\pi]$ of their respective phases. Since the color coding gives us information about the phase locations of the oscillators at $T = T_{p1}$ and $T_{p2}(T_{p1} + \tau)$, their locations at the time of echo ($T_{\text{echo}} = T_{p1} + 2\tau$) may also be predicted as long as the frequency structure of the network remains unchanged. An overlap of phases between these four groups as explained in [22] is expected at $T_{\text{echo}} = T_{p1} + 2\tau$ [panel (f)], giving rise to the increment in the order parameter. This provides a qualitative description of the subtle interplay of detuning and cluster formation that leads to the phenomenon of the echo.

As mentioned in [27–31,35–38], changing the network properties such as average degree ($\langle d \rangle$) and network randomness (β) greatly changes the spatiotemporal dynamics of a network. This leads to changes in the background order parameter of the system upon varying these network parameters. Hence, to distinguish the first echo from the background fluctuations in the order parameter of the system, a quantity called *normalized echo* (ζ) is used:

$$\zeta = \frac{R_{T_{\text{echo}}}}{\max(R_{\text{background}})}.$$

A network is considered to exhibit echo behavior only if the order parameter at the time of the echo is greater than the background fluctuations in the order parameter, i.e., $\zeta > 1$. Hence this measure helps in eliminating false identifications of echoes arising from spurious increments in $R_{T_{\text{echo}}}$ caused by an overall enhancement of the background order parameter ($R_{\text{background}}$) and ensures the identification of genuine echoes. $R_{\text{background}}$ was calculated after the transients had subsided and before the first perturbation, i.e., $400 \leqslant T \leqslant 650$ time units. Hence, the maximum value of the order parameter (R) from this time domain was considered to be the denominator in the formula for ζ.

Figure 3 shows normalized echo size ζ as a function of coupling constant C_0 in a ring network ($\beta = 0$) for four different average degrees ($\langle d \rangle > 0$), with values of $\zeta > 1$ indicating the presence of discernible echoes. We find that the network shows echo behavior, characterized by ζ when the oscillators are uncoupled (i.e., $C_0 = 0$), and continues to exhibit echoes for sufficiently weak coupling. An initial increase in echo size ζ as a result of increased coupling was observed as mentioned in [22]. However, after a critical value of coupling strength the echo size ζ starts to decrease sharply, as the system moves towards a more synchronized state [21,22]. These results are in agreement with [22], where a similar relationship was observed between coupling strength and echo size, for mean field coupling.

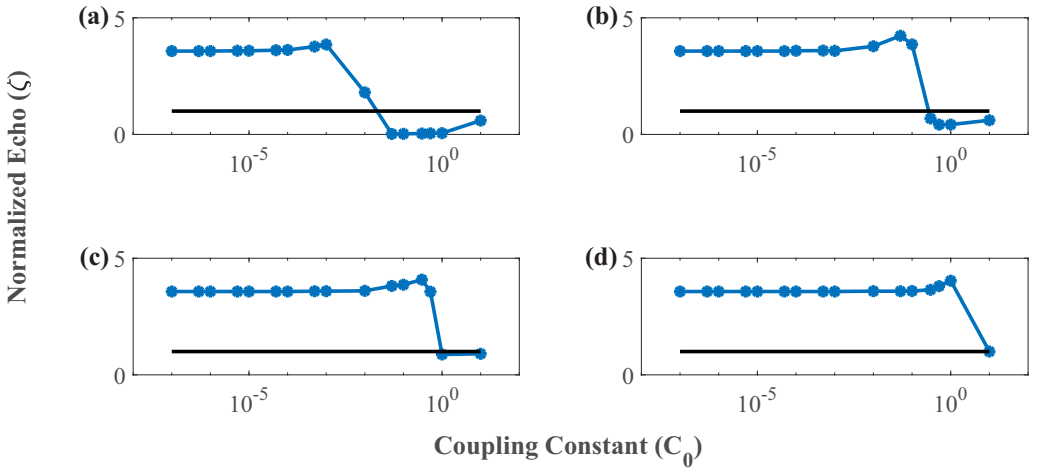

FIG. 3. Normalized echo size ζ as a function of coupling constant C_0, for a regular ring network ($\beta = 0$), with four different $\langle d \rangle$ values. The panels (a), (b), (c), and (d) correspond to $\langle d \rangle = 2$, 40, 200, and 1998, respectively. The network loses an echo after a critical value of the coupling constant (C_0^*), and this critical value depends on $\langle d \rangle$. The line $\zeta = 1$ indicates the threshold to determine an echo. Values of ζ above this line can be considered to show significant echo behavior, while $\zeta < 1$ are considered not to show an echo. The results here correspond to frequency values taken from an evenly spaced frequency distribution as mentioned in the text. Note that similar trends are also observed for frequency distributions with a Gaussian profile, i.e., frequencies taken from a Gaussian distribution and increasing monotonically as a function of oscillator index.

Since the overall synchrony of the system depends on the average degree of the underlying connection network, the critical coupling strength is also dependent on the average degree. The critical coupling strength after which a network of average degree $\langle d \rangle$ loses the echo behavior is denoted as $C_0^*(\langle d \rangle)$. We observe that $C_0^*(\langle d \rangle)$ increases approximately linearly with average degree, implying that networks with higher $\langle d \rangle$ support echoes over larger ranges of C_0 values.

To avoid network synchronization and consequent loss of echoes at a high coupling, we consider $C_0 = 0.5$ in this paper. At this coupling strength, networks with $\langle d \rangle = 2$ and 40 do not exhibit echoes, while networks with $\langle d \rangle = 200$ and 1998 yield echoes, with normalized echo size $\zeta > 3$. So this coupling constant provides a good test bed to explore the effects of network topology, as it offers contrasting baseline cases of the regular ring, yielding both $\zeta > 1$ and $\zeta < 1$ depending on the average degree of the network.

III. ECHOES IN STATIC NETWORKS

In this section, the dependence of normalized echo size (ζ) on the network properties such as average degree ($\langle d \rangle$) and randomness (β) is explored for static networks. In such networks the links are time invariant and so the randomness in connections, introduced by varying β, is frozen in time. As mentioned earlier, the parameter β is a measure of the fraction of the total number of links that are randomized, and average degree ($\langle d \rangle$) is an indicator of the average number of connections formed by an oscillator in the network. Figure 4 shows normalized echo size ζ as a function of network randomness β for networks with four different average degrees. In a conventional ring network with $\langle d \rangle = 2$, the neighboring oscillators have the least frequency difference except for the $2000 \leftrightarrow 1$ link. Upon randomizing these links, the frequency difference between two oscillators connected by a link increases, leading to a larger mutual detuning. Consequently, the overall synchrony of the system is reduced. Therefore, an increase in echo size induced by the randomized links is expected. We find that this is indeed broadly true, with the effect being most pronounced for networks of low average degrees. For instance, for the case of $\langle d \rangle = 2$ in Fig. 4(a), the regular ring fails to exhibit echoes, while sufficiently randomized networks of the same average degree yield sizable echoes. As $\langle d \rangle$ is increased, the network starts approaching a globally coupled system, where rearranging the links does not affect the underlying connection network. So changing β does not significantly affect echo size ζ for high values of $\langle d \rangle$ [see Fig. 4(d)].

While always exhibiting observable echoes, there is a subtle nonmonotonicity in the normalized echo size for $\langle d \rangle = 200$ [see Fig. 4(c)]. This stems from the fact that ζ is determined by both the order parameter at the time of echo and the background order parameter ($R_{\text{background}}$) which depends on network topology. So the nonmonotonicity of ζ can be accounted for by considering the changes in both $R_{\text{background}}$ and $R_{T_{\text{echo}}}$. We find that $R_{\text{background}}$ for this network increases sharply upon changing β from 0 to 0.1, while there is a relatively small increment in $R_{T_{\text{echo}}}$. This leads to a small overall decrement in ζ as β changes from 0 to 0.1. The rise in ζ for subsequent β values stems from the monotonic increase of $R_{T_{\text{echo}}}$ and the saturation of $R_{\text{background}}$ with increasing network randomness.

Figure 5 shows the time evolution of the order parameter for cases where an echo is present, and for illustrative contrasting scenarios where no echo is obtained. Specifically, Figs. 5(a) and 5(b) correspond to the order parameter evolution observed in typical cases of $\zeta < 1$ and $\zeta > 1$ in Fig. 3(b), and Figs. 5(c) and 5(d) correspond to that observed in typical cases of $\zeta < 1$ and $\zeta > 1$ in Fig. 4(b). The emergence of

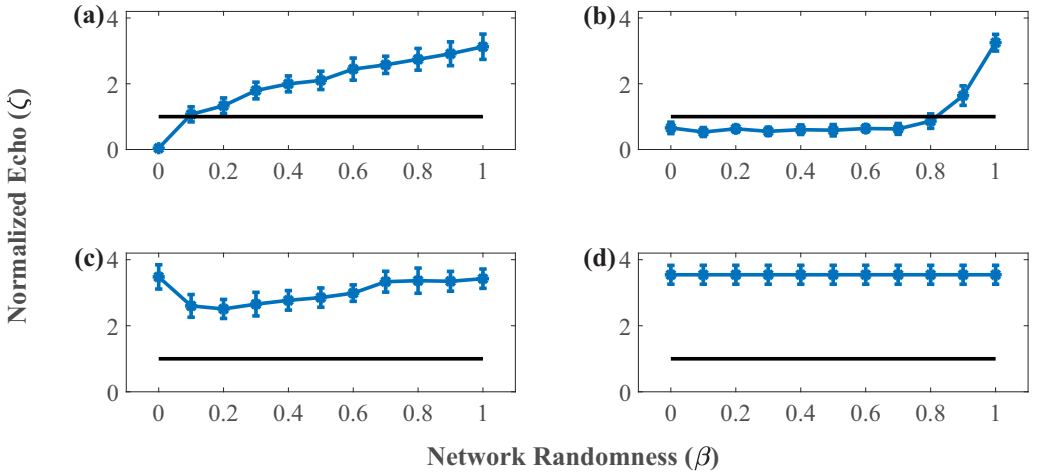

FIG. 4. Normalized echo size ζ as a function of the network randomness β, for networks with varying average degrees ($\langle d \rangle$), with coupling strength $C_0 = 0.5$. Note that a regular ring of oscillators does not yield an echo at this coupling strength for $\langle d \rangle = 2$ (a) and 40 (b) and displays echoes for $\langle d \rangle = 200$ (c) and 1998 (d). All panels show the mean ζ with error bars calculated over 20 different iterations, sampling different initial conditions and adjacency matrices. The line $\zeta = 1$ indicates the threshold below which the system is considered not to exhibit the echo behavior. A monotonic increase in ζ for increasing randomness is observed for $\langle d \rangle = 2$ and 40, while echo size is not significantly changed for $\langle d \rangle = 200$ and 1998 and always remains above 1.

echoes under increasing randomness and decreasing coupling strength is clearly evident through the time evolution of the order parameter displayed in this figure.

Now we focus specifically on the effect of the average degree of the network on echo size. Figure 6 shows the dependence of the normalized echo size ζ on the average degree ($\langle d \rangle > 0$) of the network, for various values of network randomness β. We find that there is a transition in echo size from $\zeta < 1$ to $\zeta > 1$ beyond a critical value of the average degree ($\langle d \rangle$) for $\beta = 0$, i.e.; a regular ring with average degree larger than a critical value yields echoes [Fig. 6(a)]. This result is consistent with the trends evident in Fig. 3. For $\beta = 1$ the echo size does not vary significantly with $\langle d \rangle$ and is always above 1; i.e., a completely random network always yields an echo [Fig. 6(d)]. This is intuitively expected from the fact that a completely random network has many connection shortcuts, and so is akin to a high average degree network. However, for intermediate β values, echo size ζ shows a nontrivial nonmonotonic dependence, with a minimum occurring at an intermediate value of average degree $\langle d \rangle$ [Figs. 6(b) and 6(c)]. This is due to an interplay of competing effects as mentioned in the following text. For a fixed network randomness β, the effect of reshuffling would be more significant in networks with smaller average degree as compared to networks with

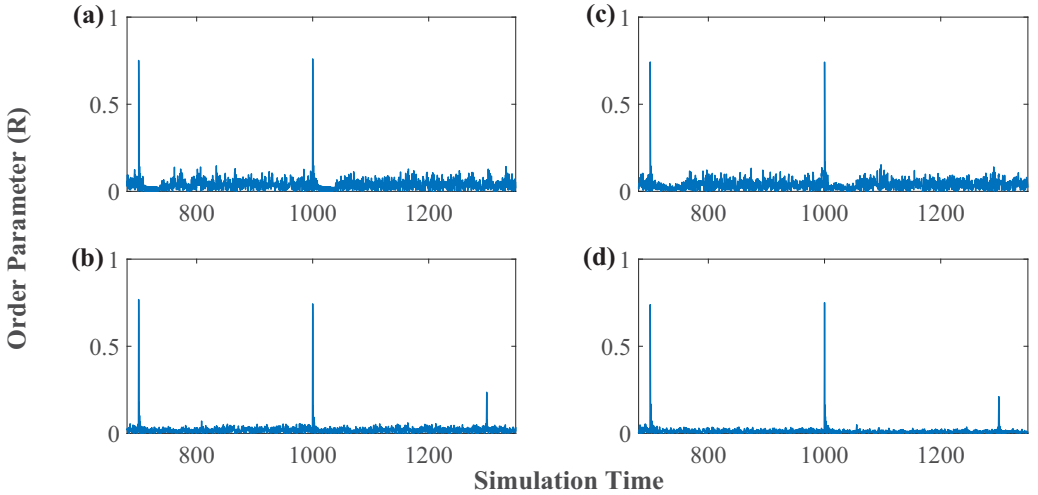

FIG. 5. Evolution of the order parameter (R) for two configurations from Figs. 3(b) and 4(b). The left panels show $R(t)$ for a ring network ($\beta = 0$) with average degree, $\langle d \rangle = 40$. (a) At high coupling constant ($C_0 = 1$), no echo was observed for this network. (b) Lowering the C_0 value to 0.01, we were clearly able to see the echo behavior. In the right panels, C_0 was fixed at 0.5 and β was varied for a network with $\langle d \rangle = 40$. (c) At $\beta = 0.7$, no echo was observed. (d) The echo emerges in the presence of sufficient randomness in the network connections (at $\beta = 1$).

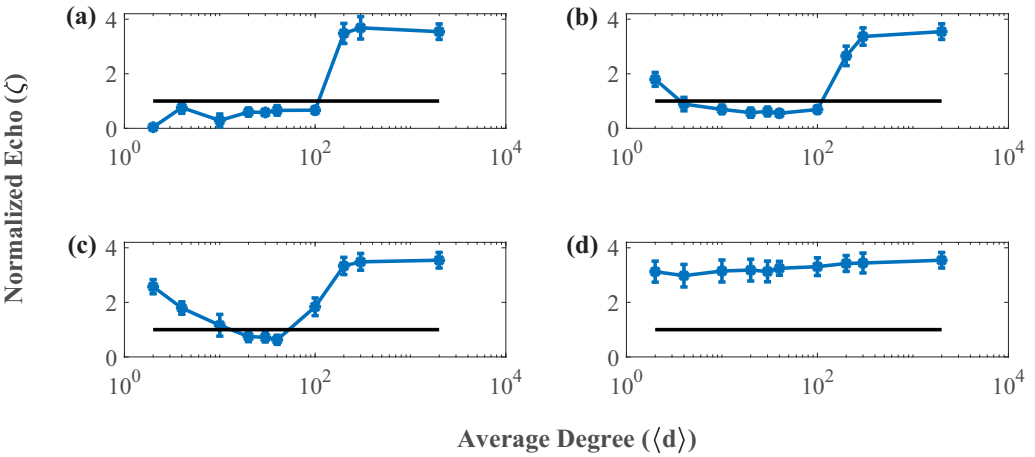

FIG. 6. Normalized echo size ζ as a function of the average degree $\langle d\rangle$ of the network, for various values of network randomness β. All the panels show the mean ζ with error bars calculated over 20 different iterations, sampling different initial conditions and adjacency matrices. The line $\zeta = 1$ indicates the threshold below which the system is considered not to exhibit the echo behavior. (a) There is a transition in echo size from $\zeta < 1$ to $\zeta > 1$ beyond a critical average degree for $\beta = 0$; i.e., a regular ring with average degree larger than a critical values yields echoes. (d) For $\beta = 1$ the echo size does not vary significantly with average degree and is always above 1; i.e., a completely random network always yields an echo. However, for intermediate β values, i.e., at $\beta = 0.3$ (b) and 0.7 (c), echo size ζ shows a nonmonotonic dependence, with a minimum occurring at an intermediate value of average degree $\langle d\rangle$.

larger average degrees. For example, if a link for a particular oscillator in a network with average degree 2 is randomized, 50% of its links are changed. In contrast, randomization of one link in a network of average degree 40 would affect only 2.5% of the coupling interaction term for that particular oscillator. In the limit of very high average degree networks, switching links will not influence the coupling term at all, as the reshuffled links will still be contained in the coupling neighborhood and included in the sum in Eq. (1). Consequently, the effective detuning of the network will be more for $\langle d\rangle = 2$ as compared to $\langle d\rangle = 40$ for the same β. Therefore, for higher average degrees, it would require larger β to observe the same amount of change in ζ as was observed for a smaller β in networks of lower average degree. This is evident from Fig. 4(b), where echoes reappear at higher randomization (specifically $\beta > 0.8$) in a network with $\langle d\rangle = 40$, as compared to a network with $\langle d\rangle = 2$ where it appears at $\beta > 0.1$. As the average degree is increased, the network starts approaching a globally coupled network. Since switching links in a network close to the globally coupled limit does not affect network topology, changing β will not significantly affect echo size ζ for high values of $\langle d\rangle$ [Fig. 4(d)].

The trends in normalized echo size ζ observed in Figs. 4 and 6 can be qualitatively rationalized by the following argument. To leading order, one expects the sum over uncorrelated contributions from random sites to reduce the magnitude of the interaction term, and this can be captured by a rescaling of the coupling strength to an effective value given by

$$C_{\text{eff}}(\langle d\rangle, \beta) \;=\; C_0\,\{1 - P_{\text{eff}}(\langle d\rangle, \beta)\} \qquad (3)$$

where C_0 is the coupling constant (equal to 0.5 in our representative examples). P_{eff} encapsulates the effective randomness introduced in a network of average degree $\langle d\rangle$ by rewiring of links, which in turn determines the effective detuning and consequent echo size. Larger network randomness β increases P_{eff}, leading to a decrement in C_{eff} and consequently an increment in echo size ζ upon increasing β. As argued earlier, average degree $\langle d\rangle$ also influences the effective coupling, as the fractional contribution of the random sites to the sum constituting the interaction term is inversely proportional to average degree; i.e., random links will have a larger effect on the sum reflecting the local interaction field, for low $\langle d\rangle$. These two opposing trends imply that

$$P_{\text{eff}} \sim f(\beta)g(\langle d\rangle)$$

where $f(\beta)$ is a monotonically increasing positive function of network randomness β, and $g(\langle d\rangle)$ is a monotonically decreasing positive function of average degree $\langle d\rangle$. So $C_{\text{eff}}(\langle d\rangle, \beta) \leqslant C_0 \quad \forall\ \beta, \langle d\rangle$. Now in order to determine if an echo will be obtained at a particular value of network randomness β and average degree $\langle d\rangle$ we need to ascertain if $C_{\text{eff}}(\langle d\rangle, \beta)$ is less than the critical coupling strength $C_0^*(\langle d\rangle)$. The first important implication of this effective picture is that if the coupling strength $C_0 < C_0^*(\langle d\rangle)$ we will continue to have echoes under random connections (i.e., for $0 < \beta \leqslant 1$), as we always have $C_{\text{eff}}(\langle d\rangle, \beta) < C_0^*(\langle d\rangle)$. This is indeed the case, and so the prediction from this analysis is consistent with the results from numerical simulations presented in Figs. 4(c) and 4(d).

The most interesting scenario arises for networks of average degree $\langle d\rangle$ where $C_0 > C_0^*(\langle d\rangle)$, as for the case of $\langle d\rangle = 2$ and 40, Now there is the possibility that large enough β, i.e., networks that are sufficiently random, will yield C_{eff} that is small enough to be lower than the critical C_0^*. For instance, networks of average degree $\langle d\rangle = 2$ and 40 do not yield echoes for regular rings ($\beta = 0$) for $C_0 = 0.5$, but support echoes for sufficiently large β. So a random network now exhibits echoes, while the regular ring with the same average degree does not.

Another significant consequence of Eq. (3) is the following: since on the one hand function $g(\langle d\rangle)$ is monotonically

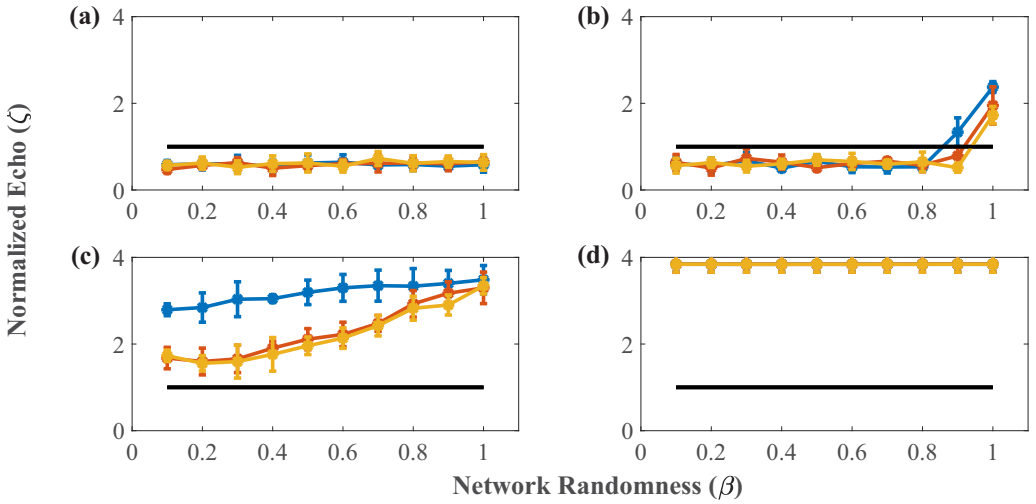

FIG. 7. Dependence of normalized echo size ζ on the network randomness β, for various $\langle d \rangle$ values. The blue, red, and yellow curves correspond to fast (1/time unit), intermediate (0.1/time unit), and slow (0.02/time unit) dynamic rewiring, respectively. (a) No echo was observed for a low average degree $\langle d \rangle = 2$ network. (b) The echo starts reappearing at high β values when the average degree is increased to 40. (c) A monotonic increment in ζ is observed for $\langle d \rangle = 200$. (d) No change in ζ is observed upon changing the β for a network of average degree 1998. For each switching rate, the panels show the mean ζ with error bars calculated over seven different iterations, sampling different initial conditions and dynamic adjacency matrices.

decreasing, thus detrimental to echo size, but on the other hand $C_0^*(\langle d \rangle)$ increases with average degree aiding echoes, the dependence of echo size on average degree can be nonmonotonic. A manifestation of this analysis is the observation in simulations of echoes arising in a smaller range of β for higher average degree networks [cf. Figs. 4(a) and 4(b)]. Further, for intermediate β there is a range of average degrees for which the echoes are suppressed [cf. Figs. 6(b) and 6(c)]. So the subtle interplay and balance of the two opposing trends of average degree on echo size give rise to the nontrivial dependence of the echo size on the average degree of the network. Note that the dependence of other network parameters, such as the mean path length and clustering coefficient, on average degree is monotonic. Hence we expect that the broad trends of echo size as a function of these other network parameters will also be qualitatively similar to that observed for average degree.

IV. ECHOES IN DYNAMICALLY REWIRED NETWORKS

Lastly, we focus on the robustness of echoes in dynamically rewired networks. In the dynamic network paradigm, the underlying connection network is rewired in time, with the links switched periodically keeping the fraction of random links invariant. A fast switching dynamic network is defined to be the one in which the links are reshuffled once every time unit, i.e., at a switching rate of 1/time unit. An intermediate switching rate would be 0.1/time unit. A slowly changing network rewires at the frequency of 0.02/time unit. We explore the echo size in networks rewired at fast, intermediate, and slow switching rates.

In Fig. 7, the dependence of the normalized echo size ζ on network randomness β is explored for these dynamic networks of varying average degrees. The three colors of plots correspond to fast (blue), intermediate (red), and slow (yellow) switching rates of the networks. Figure 7(a) shows that a dynamic network does not exhibit any observable echo for networks of average degree $\langle d \rangle = 2$. This is in contrast to the observation for static networks [Fig. 4(a)]. The frequency structure of the oscillators and hence the determinism regarding the positions of various groups at the time of echo are destroyed during the rewiring process. For a high average degree [Fig. 7(d)], the dynamical rewiring does not change the network connections significantly. Hence, the qualitative trend for the high average degree dynamic network is the same as its static counterpart [Fig. 4(d)]. Networks with low average degrees ($\langle d \rangle = 2$) are most affected by the dynamical rewiring because of the low number of nearest neighbor connections, which makes these network most susceptible to the destruction of frequency structure upon rewiring.

Figure 8 presents the dependence of ζ on the average degree $\langle d \rangle$ of the system for different β values under the dynamic rewiring scheme. The color scheme for the switching rates is the same as in Fig. 7. Normalized echo size ζ exhibits a smooth monotonic rise as the average degree $\langle d \rangle$ is increased for different levels of network randomness (β). Dynamically rewired networks are different from their static counterparts (Fig. 6) for low average degrees as discussed earlier.

One can also rationalize the trends in dynamically rewired networks through the same qualitative picture introduced for static networks. The crucial difference now is the following: unlike the case of static connections, switched links effectively allow each site to have short-term connections with almost every other site in the system. So the effective randomness P_{eff} is now only a monotonically increasing function of the network randomness β. Again, in order to determine if an echo will be obtained at a particular value of network randomness β and average degree $\langle d \rangle$, we need to ascertain if $C_{\text{eff}}(\beta)$ is less than the critical coupling strength $C_0^*(\langle d \rangle)$. By

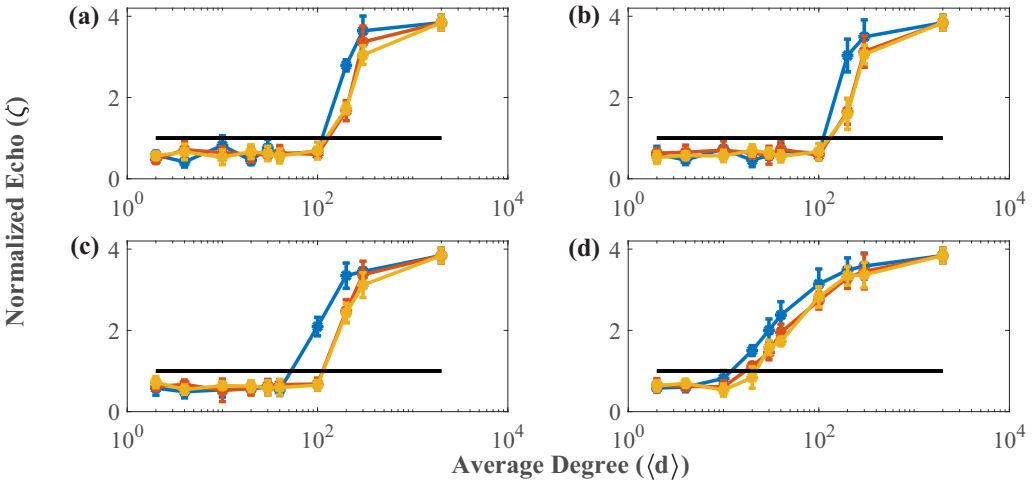

FIG. 8. Normalized echo size ζ as a function of the average degree of a network ($\langle d \rangle$) for various β values. The blue, red, and yellow curves correspond to fast (1/time unit), intermediate (0.1/time unit), and slow (0.02/time unit) dynamic rewiring, respectively. Echo starts reappearing as the average degree of a network is increased. The panels (a), (b), (c), and (d) correspond to β values equal to 0.1, 0.3, 0.7, and 1, respectively. (d) For completely random networks ($\beta = 1$), the echo reemerges at lower average degrees. For each switching rate, the panels show the mean ζ with error bars calculated over seven different iterations, sampling different initial conditions and dynamic adjacency matrices.

arguments similar to that in the static case, if coupling strength $C_0 < C_0^*(\langle d \rangle)$ we will continue to have echoes under random coupling, as $C_{\text{eff}}(\beta)$ is always less than or equal to $C_0^*(\langle d \rangle)$. This is consistent with the results from numerical simulations presented in Figs. 7(c) and 7(d).

The crucial difference between static and dynamically rewired networks arises in the dependence of echo size on the average degree of the network. Now the effective coupling C_{eff} has no significant dependence on average degree. So the dependence of echoes on average degree is determined by the dependence of $C_0^*(\langle d \rangle)$ on $\langle d \rangle$, which is approximately a linearly increasing function as mentioned earlier. An important consequence of this is that the dependence of ζ on average degree is monotonic in dynamically rewired networks (see Fig. 8), in contrast to the nonmonotonicity arising in static networks (see Fig. 6).

V. DISCUSSION

The remarkable and subtle echo phenomenon has been seen and theoretically understood in large populations of globally coupled or uncoupled oscillators [21,23–25]. However, experimental observations of echoes are sparse [22,39]. In order to assess the potential observability of the echo phenomenon in natural and engineered contexts, it is crucial that its presence in wide-ranging complex systems is investigated. Given the ubiquity of networks, this paper attempts a comprehensive understanding of echoes in networks. Specifically, we aimed to determine if the echo behavior is robust in the presence of random coupling connections and for average degrees much lower than the global coupling limit. In the case of a regular ring topology with a low average degree of connectivity, a discernible echo was not observed. Varying either of the two aforementioned parameters in such networks yields an echo. Increasing the network randomness by increasing β leads to a reemergence of echo behavior. Also, increasing the average degree beyond a critical value was found to give rise to an echo. Completely random static networks ($\beta = 1$) were found to exhibit echoes for networks of all average degrees. This suggests that randomizing links helps in inducing echoes in systems even when the average degree of connections is very low. For intermediate randomness, the system exhibits a nonmonotonic dependence of the echo size on average degree. The echo size was found to be minimum at an intermediate average degree. Given the widespread nature of dynamic networks, we have considered the influence of dynamically changing links on the echo size. The time-varying connections lead to a destruction of the echo in low average degree networks. However, the echo was observed to be robust under dynamic links in high average degree networks.

We now indicate some interesting questions that still remain open regarding the echo phenomenon. To the best of our knowledge, echoes have not been explored in collections of chaotic systems. Given the ubiquity of aperiodic dynamics in nature, it will be an exciting prospect to search for echoes in networks of chaotic oscillators. The other relevant issue is the influence of the frequency distribution on the emergence of echoes, as frequency distributions often have significant effect on emergent spatiotemporal phenomena. For example, uniform frequency distributions have been shown to exhibit a first order transition to the synchronized state in Kuramoto phase oscillators, whereas unimodal distributions show a second order transition [40]. The evenly spaced frequency distribution considered in our paper is a particular realization of the uniform distribution, and it would be interesting to analyze the effect of different classes of frequency distributions on the echo size observed in complex networks of regular or chaotic oscillators.

We conclude by summarizing our salient results. Our simulations indicate that the potential observability of echoes in real world experimental systems would depend sensitively on the average degree and randomness of the underlying

connection network, and also the time dependence of the links. Since we demonstrate that the echo behavior is predominantly limited to networks with high average degree, high randomness, and low coupling strengths, our results clearly demarcate the class of oscillator networks that are good candidates for exhibiting echoes. This will, in our opinion, help to guide experiments seeking to find the echo behavior, and to interpret the existence, or lack thereof, of the phenomenon in the real world.

ACKNOWLEDGMENTS

R.P. and P.P. would like to thank Department of Science and Technology (DST) (India), (Project No. EMR/2016/000275) for financial assistance. R.P. would also like to acknowledge Council of Scientific and Industrial Research (CSIR) (India) for financial assistance. S.S. would like to acknowledge support from the J.C. Bose Fellowship (Grant No. SB/S2/JCB-013/2015).

[1] J. P. Crutchfield, and K. Kunihiko, *Directions in Chaos* (World Scientific, Singapore, 1987).

[2] H. Chate and P. Manneville, Prog. Theor. Phys. **87**, 1 (1992).

[3] D. M. Abrams and S. H. Strogatz, Phys. Rev. Lett. **93**, 174102 (2004).

[4] C. Meena, K. Murali, and S. Sinha, Int. J. Bifurcation Chaos **26**, 1630023 (2016).

[5] G. C. Sethia, A. Sen, and G. L. Johnston, Phys. Rev. E **88**, 042917 (2013).

[6] M. R. Tinsley, S. Nkomo, and K. Showalter, Nat. Phys. **8**, 662 (2012).

[7] A. M. Hagerstrom, T. E. Murphy, R. Roy, P. Hövel, I. Omelechenko, and E. Schöll, Nat. Phys. **8**, 658 (2012).

[8] V. Resmi, G. Ambika, R. E. Amritkar, and G. Rangarajan, Phys. Rev. E **85**, 046211 (2012).

[9] R. Phogat, I. Tiwari, P. Kumar, M. Rivera, and P. Parmananda, Eur. Phys. J. B **91**, 111 (2018).

[10] S. S. Chaurasia, M. Yadav, and S. Sinha, Phys. Rev. E **98**, 032223 (2018).

[11] U. K. Verma, S. S. Chaurasia, and S. Sinha, Phys. Rev. E **100**, 032203 (2019).

[12] R. Phogat and P. Parmananda, Chaos: An Interdisciplinary Journal of Nonlinear Science **28**, 121105 (2018).

[13] A. Pikovsky, M. Rosenblum, and J. Kurths, *Synchronization: A Universal Concept in Nonlinear Sciences* (Cambridge University, Cambridge, England, 2003).

[14] P. Kumar and P. Parmananda, Chaos: An Interdiscip. J. Nonlinear Sci. **28**, 045105 (2018).

[15] P. Parmananda, B. J. Green, and J. L. Hudson, Phys. Rev. E **65**, 035202(R) (2002).

[16] M. Rivera, P. Parmananda, and M. Eiswirth, Phys. Rev. E **65**, 025201(R) (2002).

[17] P. K. Shaw, M. S. Janaki, A. N. S. Iyengar, T. Singla, and P. Parmananda, Chaos, Solitons and Fractals **78**, 256 (2015).

[18] M. Nurujjaman, A. N. Sekar Iyengar, and P. Parmananda, Phys. Rev. E **78**, 026406 (2008).

[19] T. R. Chigwada, P. Parmananda, and K. Showalter, Phys. Rev. Lett. **96**, 244101 (2006).

[20] P. Parmananda, H. Mahara, T. Amemiya, and T. Yamaguchi, Phys. Rev. Lett. **87**, 238302 (2001).

[21] E. Ott, J. H. Platig, T. M. Antonsen, and M. Girvan, Chaos: An Interdiscip. J. Nonlinear Sci. **18**, 037115 (2008).

[22] T. Chen, M. R. Tinsley, E. Ott, and K. Showalter, Phys. Rev. X **6**, 041054 (2016).

[23] M. Herrera, T. M. Antonsen, E. Ott, and S. Fishman, Phys. Rev. A **86**, 023613 (2012).

[24] E. Ott, J. Plasma Phys. **4**, 471 (1970).

[25] R. Gould, T. M. O'neil, and J. H. Malmberg, Phys. Rev. Lett. **19**, 219 (1967).

[26] D. J. Watts and S. H. Strogatz, Nature (London) **393**, 440 (1998).

[27] S. Sinha, Phys. Rev. E **66**, 016209 (2002).

[28] A. Mondal, S. Sinha, and J. Kurths, Phys. Rev. E **78**, 066209 (2008).

[29] F. Varela, J. P. Lachaux, and J. Martinerie, Nat. Rev. Neurosci. **2**, 229 (2001).

[30] V. Brezina, I. V. Orekhova, and K. R. Weiss, J. Neurophysiol. **83**, 207 (2000).

[31] C. Von der Malsburg, *Dynamic Link Architecture* (MIT, Cambridge, MA, 2002).

[32] V. M. Eguiluz, D. R. Chialvo, G. A. Cecchi, M. Baliki, and A. V. Apkarian, Phys. Rev. Lett. **94**, 018102 (2005).

[33] A. Wagner and D. A. Fell, Proc. R. Soc. B **268**, 1803 (2001).

[34] B. Uzzi and J. Spiro, Am. J. Soci. **111**, 447 (2005).

[35] P. D. Rungta, A. Choudhary, C. Meena, and S. Sinha, Europhys. Lett. **117**, 20003 (2017).

[36] C. Mitra, A. Choudhary, S. Sinha, J. Kurths, and R. V. Donner, Phys. Rev. E **95**, 032317 (2017).

[37] A. Choudhary, C. Mitra, V. Kohar, S. Sinha, and J. Kurths, Chaos: An Interdiscip. J. Nonlinear Sci. **27**, 111101 (2017).

[38] P. D. Rungta, C. Meena, and S. Sinha, Phys. Rev. E **98**, 022314 (2018).

[39] R. M. Hill and D. E. Kaplan, Phys. Rev. Lett. **14**, 1062 (1965).

[40] D. Pazó, Phys. Rev. E **72**, 046211 (2005).